Mutation-oriented profiling of autoinhibitory kinase conformations predicts RAF inhibitor efficacies

Johanna E. Mayrhofer[a,1], Florian Enzler[a,b,1], Andreas Feichtner[a], Ruth Röck[a], Jakob Fleischmann[a], Andrea Raffeiner[a], Philipp Tschaikner[a,c], Egon Ogris[d], Roland G. Huber[e], Markus Hartl[a], Rainer Schneider[a], Jakob Troppmair[b], Omar Torres-Quesada[a,2], and Eduard Stefan[a,2]

[a]Institute of Biochemistry and Center for Molecular Biosciences, University of Innsbruck, 6020 Innsbruck, Austria; [b]Daniel Swarovski Research Laboratory, Department of Visceral, Transplant and Thoracic Surgery, Medical University of Innsbruck, 6020 Innsbruck, Austria; [c]Institute of Molecular Biology, University of Innsbruck, 6020 Innsbruck, Austria; [d]Center for Medical Biochemistry, Max Perutz Labs, Medical University of Vienna, A-1030 Vienna, Austria; and [e]Bioinformatics Institute, Agency for Science Technology and Research, 138671 Singapore, Singapore

Edited by Melanie H. Cobb, University of Texas Southwestern Medical Center, Dallas, TX, and approved October 14, 2020 (received for review June 17, 2020)

Kinase-targeted therapies have the potential to improve the survival of patients with cancer. However, the cancer-specific spectrum of kinase alterations exhibits distinct functional properties and requires mutation-oriented drug treatments. Besides post-translational modifications and diverse intermolecular interactions of kinases, it is the distinct disease mutation which reshapes full-length kinase conformations, affecting their activity. Oncokinase mutation profiles differ between cancer types, as it was shown for BRAF in melanoma and non–small-cell lung cancers. Here, we present the target-oriented application of a kinase conformation (KinCon) reporter platform for live-cell measurements of autoinhibitory kinase activity states. The bioluminescence-based KinCon biosensor allows the tracking of conformation dynamics of full-length kinases in intact cells and real time. We show that the most frequent BRAF cancer mutations affect kinase conformations and thus the engagement and efficacy of V600E-specific BRAF inhibitors (BRAFi). We illustrate that the patient mutation harboring KinCon reporters display differences in the effectiveness of the three clinically approved BRAFi vemurafenib, encorafenib, and dabrafenib and the preclinical paradox breaker PLX8394. We confirmed KinCon-based drug efficacy predictions for BRAF mutations other than V600E in proliferation assays using patient-derived lung cancer cell lines and by analyzing downstream kinase signaling. The systematic implementation of such conformation reporters will allow to accelerate the decision process for the mutation-oriented RAF-kinase cancer therapy. Moreover, we illustrate that the presented kinase reporter concept can be extended to other kinases which harbor patient mutations. Overall, KinCon profiling provides additional mechanistic insights into full-length kinase functions by reporting protein–protein interaction (PPI)-dependent, mutation-specific, and drug-driven changes of kinase activity conformations.

precision medicine | biosensor | drug efficacy prediction | mutant BRAF | lung cancer

The identification of genetic alterations in signaling pathways that drive tumor etiology and progression has promoted targeted cancer therapy approaches. Tumor genotyping identifies cancer-driver mutations and suggests therapeutic strategies to benefit patients. Distinct genetic alterations of the particular tumor type enable precision medicine efforts involving the administration of effective chemical inhibitors to antagonize oncoprotein functions. One of the most frequently targeted enzyme families is the kinase one (1–4). Cancer genotyping along with mechanistic insights into kinase functions have unveiled that heterogeneous kinase mutations promote and relay diverse signaling outputs. The current challenge is to connect these findings with tailored drug development and discovery approaches to apply "the perfect drug." In the past decade, the genotype-directed management of the deregulated mitogen-activated protein kinase (MAPK) pathway harboring distinct pathway mutations has emerged as a paradigm for kinase-directed precision oncology (5, 6). The first MAPK in this pathway is represented by the RAF family kinases, with oncogenic mutations predominantly found in the BRAF isoform (6–10). RAF activation depends on the protein interaction with the GTP-loaded GTPase RAS (11). The consequences are membrane recruitment, phosphorylation, and the subsequent release of the autoinhibitory BRAF configuration, resulting in a shift into active kinase conformation (9, 12–14). BRAF mutations have been identified in several cancer types, such as malignant melanomas (50 to 60%), thyroid (30 to 50%), colorectal (10%), and lung (3%) cancers (15, 16). The most common gain of function mutation in BRAF in malignant melanomas (>90%) is the V600E substitution (6). Selective inhibitors of BRAF-V600E have been approved for the treatment of metastatic melanomas (vemurafenib [PLX4032] and dabrafenib [GSK2118436A]) and show profound clinical responses in patients (16, 17). Besides other types of RAFi combination therapies with MEK inhibitors (MEKi), one poly-pharmacology approach using encorafenib (LGX818) and binimetinib (MEKi) has been approved in 2018 for the treatment of patients with

Significance

The pharmaceutical targeting of mutated BRAF has shown promising clinical outcomes in patients with melanoma. However, more than 300 reported BRAF patient mutations and the occurrence of a kinase-drug resistance mechanism hamper patient-oriented therapies. We have developed an extendable and cell-based kinase conformation reporter platform (KinCon) to predict and compare the effect of kinase drugs. We systematically evaluated drug efficacies by assessing KinCon reporter dynamics in response to different drugs and patient mutations. Our findings suggest that FDA-approved melanoma inhibitors may have the potential to block non-V600E–mutated BRAF activities also in non–small-cell lung cancers (NSCLC). We assume that widespread analyses of KinCon:drug interactions may assist in the future in identifying patient mutation–specific and thus more effective kinase inhibitors.

Author contributions: E.S. designed research; J.E.M., F.E., A.F., R.R., J.F., A.R., P.T., R.G.H., M.H., and O.T.-Q. performed research; E.O. and J.T. contributed new reagents/analytic tools; J.E.M., F.E., A.F., R.R., J.F., A.R., P.T., E.O., R.G.H., M.H., R.S., J.T., O.T.-Q., and E.S. analyzed data; and E.S. wrote the paper.

Competing interest statement: Aspects of the present study are subject to pending patent applications.

This article is a PNAS Direct Submission.

This open access article is distributed under Creative Commons Attribution-NonCommercial-NoDerivatives License 4.0 (CC BY-NC-ND).

[1]J.E.M. and F.E. contributed equally to this work.

[2]To whom correspondence may be addressed. Email: omar.quesada@uibk.ac.at or eduard.stefan@uibk.ac.at.

This article contains supporting information online at https://www.pnas.org/lookup/suppl/doi:10.1073/pnas.2012150117/-/DCSupplemental.

First published November 23, 2020.

Downloaded by guest on December 15, 2020

metastatic melanoma involving BRAF-V600E/K mutations (18). However, one needs to note that the duration of the antitumor response of this treatment is variable and the efficacy of the inhibitors is limited because of the onset of drug resistance (16, 19–21).

So far, nearly 300 distinct missense mutations of BRAF have been identified (22, 23). In addition to strongly activating mutations, some amino acid exchanges lead to intermediate or low kinase activity. These mutations primarily occur within the activation- or in the phosphate-binding loops of the protein kinase. Overall, the biochemistry of BRAF mutants varies substantially. In contrast to melanomas, several studies underline that in non–small-cell lung cancers (NSCLC), non–BRAF-V600E mutations account for more than 50% of mutations, with the major mutation burden of G466, G469, K601, N581, and D594 substitutions (24–29). The effect of these non-V600E mutations is not fully understood, but they have been implied to be responsible for alterations of the kinase conformation, enhancement of RAF dimerization, mimicking of kinase autophosphorylation, or the ordering of the hydrophobic kinase R spine (9, 22, 30–32). Here, we present a modular and extendable reporter platform which is applicable for noninvasive recordings of opened and closed protein kinase conformations (KinCon reporter) in the context of assessing kinase drug efficacies.

Results

Kinase Conformation Dynamics. Proteins are dynamic entities that undergo conformational rearrangements that are tightly related to their biological functions (30, 33, 34). A variety of critical signaling proteins display diverse types of conformational changes as part of their activity cycles. Alterations of intramolecular interactions activate or inactivate the protein function (35–38). The simplest way to achieve protein inhibition in *cis* is the intramolecular binding of autoinhibitory modules (AIM) to functional protein domains, which can be of a different kind (36). Conformational transitions are initiated by binding events, different means of post-translational modifications (PTM), or AIM proteolysis. Besides binary complex formation of autoinhibitory proteins with other macromolecules, AIM-mediated protein dynamics involve molecular high-affinity interactions with ligands, cofactors, metabolites, or drugs (6, 9, 39–41). Thus, it is necessary to record the molecular motions of AIM-containing full-length proteins directly in the appropriate cellular setting. Adaptable biosensor technologies for intramolecular protein dynamics are still missing. We engineered genetically encoded biosensors to quantify autoinhibitory conformation changes of kinases and other signaling proteins involved in oncogenic signaling (13, 42).

First, we used a recently published computational prediction tool to identify potential cis-regulatory elements (CREs) in the protein kinase family. The human kinases were retrieved from the Uniprot database and were then assigned to their respective classes. Furthermore, the sequences of all kinases were then processed by the Cis-regPred algorithm for the presence of CREs (http://aimpred.cau.ac.kr) (36). *SI Appendix*, Table S1 shows the number and the amino acid coordinates of CREs identified within each kinase sequence. Out of ∼600 screened kinase sequences, 270 contained predicted CREs (red- and black-labeled kinases in the kinome tree; Fig. 1*A*). Red labeling signifies the kinases which we tested with the conformation reporter (43, 44).

Full-Length BRAF Conformations and Cancer Mutations. This study focuses on the MAPK pathway, which is the most commonly mutated kinase signaling cascade in cancer (5). As a starting point, we selected the oncogenic RAF kinase isoform BRAF. Oncogenic mutations in BRAF lead to regulation-uncoupled phosphorylation events (1, 5, 45). The biochemistry of the BRAF mutants varies substantially with regard to activity, interactions, and responsiveness to phosphotransferase inhibition. FRET and BRET reporters have been described for measuring RAF kinase protein–protein interactions (PPI) and dynamics (14, 46, 47). We set out to apply a protein-fragment complementation assay (PCA)–based kinase conformation (KinCon) reporter platform to systematically record the impact of combinations of mutations and approved kinase inhibitors or lead molecules on enzyme activity conformations (13, 42). We integrated the most frequent BRAF cancer patient mutations into the KinCon platform for tailored drug discovery efforts to be performed directly in the target cell. We took advantage of an intramolecular PCA which consists of the full-length BRAF N-terminally tagged with fragment 1 (F[1]-) and C-terminally fused to fragment 2 (-F[2]) of the *Renilla* luciferase (*R*luc) to generate the KinCon reporter F[1]-BRAF-F[2] (13, 48, 49). We assumed that in the inactive state, this wild-type BRAF reporter adopts the closed full-length conformation. The N-terminal AIM inhibits the C-terminal kinase domain by binding, as indicated in the KinCon reporter design principle shown in Fig. 1*B*. RAS activation, RAF mutations, kinase inhibitor binding, or molecular interactions may affect KinCon conformations by interconverting between closed and opened kinase states. This is reflected by alterations of bioluminescence signals emitted by reconstituted *R*luc (Fig. 1*B*).

In coexpression experiments with wild-type HRAS and HRAS-G12V in human embryonic kidney 293 (HEK293) cells, we observed opening of the BRAF conformation reporter in the presence of GTP-loaded HRAS, as predicted (Fig. 1 *C*, *Left*) (13). Next, we activated endogenous epidermal growth factor (EGF) receptors with the EGF peptide to record the immediate effect of upstream pathway activation (5- and 10-min agonist exposure) on BRAF KinCon conformation changes. We showed that EGF treatments of HEK293 cells induce MEK and ERK phosphorylation/activation (*SI Appendix*, Fig. S1*A*). We observed a drop in emitted bioluminescence which was caused by EGF-initiated GTP loading of coexpressed HRAS and the subsequent BRAF interaction, shifting the wild-type BRAF KinCon reporter to a more opened kinase conformation (Fig. 1 *C*, *Right*). In the case of coexpressed HRAS-G12V, the KinCon reporter was already partially opened and thus less responsive to EGF stimulation (Fig. 1*C*). So far, nearly 300 distinct missense mutations of BRAF have been identified in tumor samples and cancer cell lines (22, 23). Most of the mutations occur in the activation (A loop) or in the phosphate-binding loops (P loop) (Fig. 1*D*). We have selected mutations of BRAF according to the frequency of their appearance in cancer cell lines or tumors (Fig. 1*D*) (9, 50). We used a site-directed mutagenesis approach to construct BRAF KinCon reporter harboring the patient mutations G466V, G469A, Y472C, N581S, D594G, L597V, V600E, V600K, V600R, and K601E. These mutations show distinct kinase activity states (Fig. 1 *D*, *Right*). The phosphotransferase states of tested BRAF mutations have all been recently classified by Yao and colleagues with high, low, intermediate, and no kinase activities (50, 51). Y472C was classified in a different publication (51). First, we overexpressed each reporter in HEK293 cells to measure basal KinCon bioluminescence and determine the different KinCon protein expression levels. Next, we normalized the relative light units on KinCon reporter expression levels to obtain the expression-corrected bioluminescence signals (Fig. 1*E*) (*SI Appendix*, Fig. S1*B*). We observed a reduced bioluminescence signal, underlining a mutation-driven shift to a more opened BRAF kinase conformation, with all tested patient-derived BRAF mutations (Fig. 1*E*). Interestingly, mutations in both kinase loops, the P loop (G466V, G469A) and the A loop (N581S and V600E/K/R), showed the strongest effect. Others showed a less prominent shift toward a more opened kinase conformation. In agreement with the recent classification of BRAF mutations (50), we confirmed

Downloaded by guest on December 15, 2020

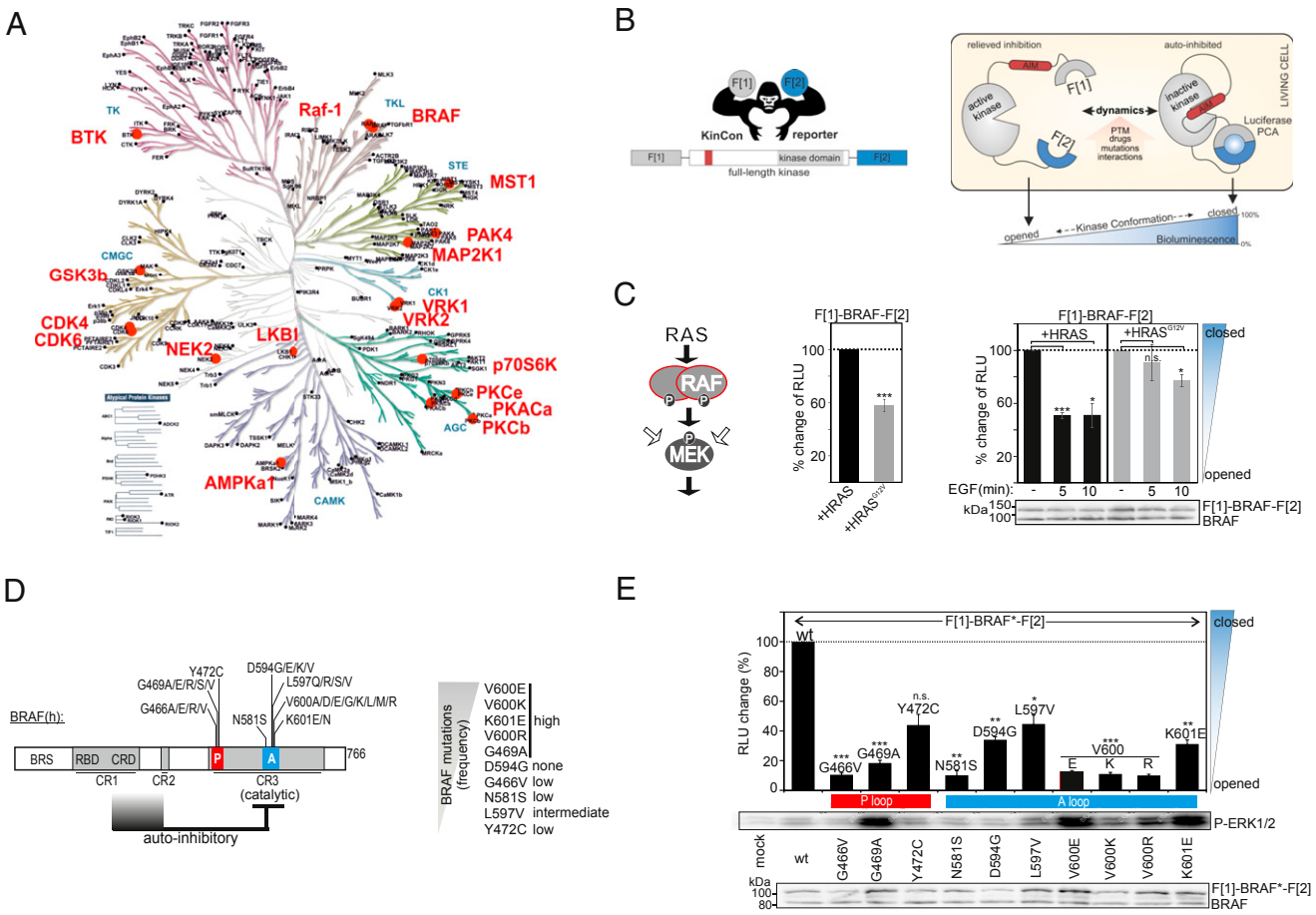

Fig. 1. Kinase conformations and BRAF KinCon reporter dynamics. (*A*) The kinases predicted to contain CREs are highlighted in the kinome tree in black and red. Red-labeled full-length kinases have been tested using the KinCon reporter system. (*B*) A schematic depiction of the KinCon reporter principle indicating fragment (1)/(2) = F-[1]/-F[2] of the *R*luc PCA with intervening GGGGSGGGGS linker. A depiction of the intramolecular KinCon reporter which contains an exemplarily AIM for kinase inhibition is shown. Indicated factors affect transitions between opened and closed full-length kinase conformations, which may result in an increase or decrease of *R*luc-PCA–emitted bioluminescence. (*C*) The effect of HRAS variant coexpression on BRAF conformations (±SEM, $n = 6$; normalized on reporter expression; *Left*). Effects of 5 and 10 min EGF (200 ng/mL) exposure on BRAF conformations in the presence of indicated HRAS variants are shown (±SEM; $n = 4$ independent experiments; *Right*; RLU, relative light units). (*D*) A schematic depiction of the modular structure of BRAF; patient mutations in the A-loop and P-loop are indicated (BRS, BRAF specific sequence; CR, conserved regions; RBD, RAS-binding domain; CRD, cysteine-rich domain). The frequencies and consequences of selected patient mutations are specified. (*E*) Shown are the expression normalized values for BRAF KinCon reporter conformations in percent of RLU (±SEM from at least $n = 4$ independent experiments). A Student's *t* test was used to evaluate statistical significance. $^*P < 0.05$, $^{**}P < 0.01$, and $^{***}P < 0.001$. n.s., nonsignificant.

that the BRAF KinCon reporter with the mutations G469A, L597V, V600E/K/R, and K601E show the strongest elevation of P-ERK1/2 levels when compared with the wild-type BRAF reporter (Fig. 1*E*).

In cell transformation assays, we confirmed that the N- and C-terminal–tagged BRAF-V600E KinCon reporter still retains oncogenic potential when compared with the higher expressed hemagglutinin (HA)-tagged BRAF variants and the cancer driver MYC (*SI Appendix*, Fig. S1*C*).

Drug Efficacy Profiling Using the BRAF KinCon Reporter. The molecular characterization of distinct tumors and cancer cell lines by sequencing has led to the identification of onco-kinases and their mutations. Biopsy genotyping has become indispensable for a precision medicine–oriented therapy in recent years. These efforts unveiled striking differences in the incidence rates of BRAF mutations in distinct cancers. In a recent large-scale study focusing on the identification of hot-spot mutations in thousands of tumors, major differences in BRAF mutation frequencies of melanoma and lung adenocarcinoma have been identified (25). In Fig. 2*A*, we present pie charts for BRAF mutation frequencies in melanoma and in lung adenocarcinoma. It is evident that the relative contribution of V600E mutations is much less pronounced in the latter.

We recently demonstrated that α-C-OUT BRAF inhibitors (BRAFi) show an allosteric effect on mutated and full-length BRAF-V600E conformations. We showed that the recorded conformational change reflects enzyme activities with the BRAF-V600E KinCon reporter (13, 42). These KinCon reporter activity profiles directly correlate with activity measurements of ERK kinase activation (13). We set out to test the reporter system with non-V600E mutations for predicting BRAFi drug efficacies. In addition to the wild-type, we subjected 10 different BRAF KinCon reporters harboring the patient-derived mutations G466V, G469A, Y472C, N581S, D594G, L597V, V600E, V600K, V600R, and K601E to BRAFi profiling experiments. We tested the α-C-OUT BRAFi which are either in the clinic (vemurafenib, dabrafenib, and encorafenib) or in preclinical trials (PLX8394) (6, 16). The KinCon profiling experiments revealed a transition to a more closed kinase conformation in 9 out of 10 mutant reporters upon exposure to 100 nM and 1 μM BRAFi (α-C-OUT inhibitor). We showed the impact of

Downloaded by guest on December 15, 2020

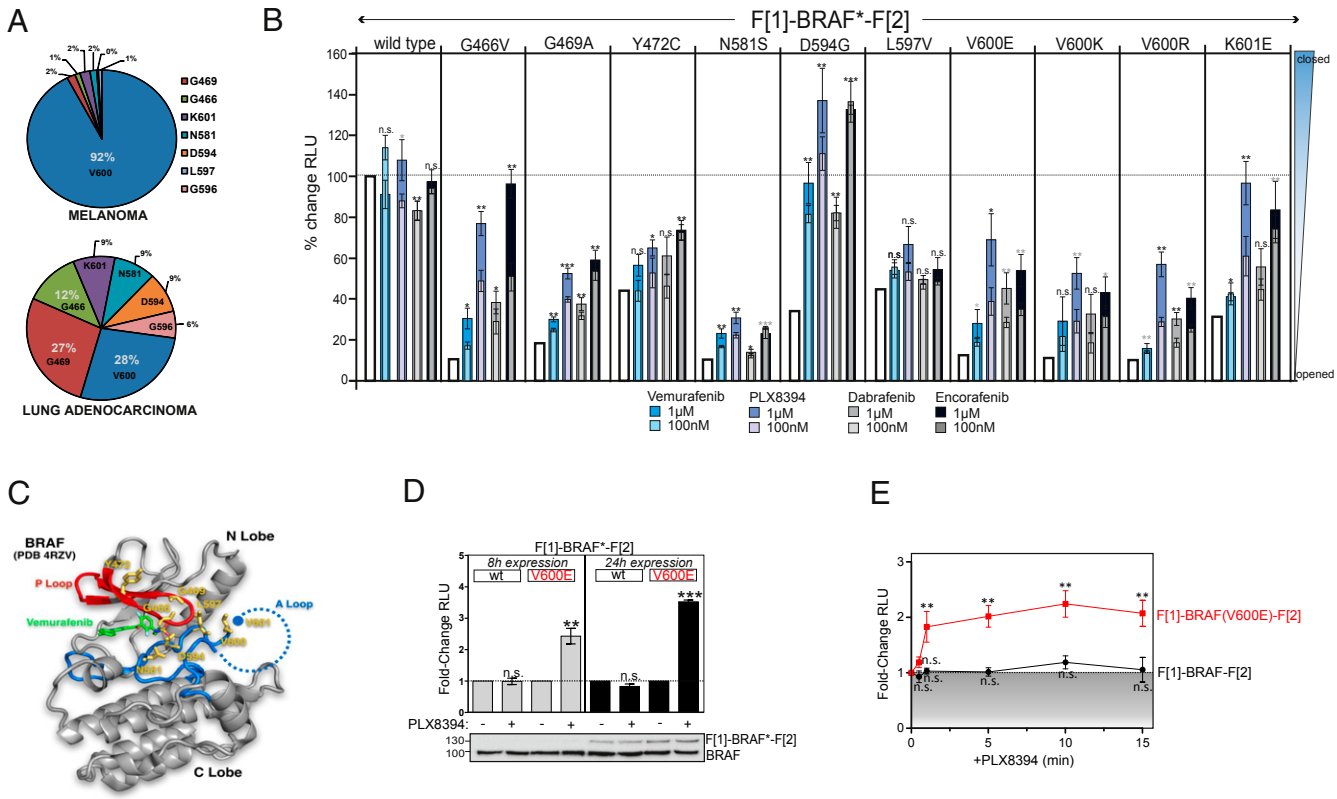

Fig. 2. Profiling of BRAF KinCon reporter dynamics upon BRAFi exposure. (*A*) A pie chart showing the BRAF mutation frequencies in melanoma and lung cancer adenocarcinoma. Data were extracted from ref. 25. (*B*) PCA measurements of BRAFi-initiated alterations of BRAF conformations using indicated BRAF KinCon reporter. BRAFi were applied for 3 h in a concentration of 100 nM and 1 μM to transiently transfected HEK293 cells (±SEM from at least $n = 4$ independent experiments). We have normalized the emitted RLU on the KinCon reporter expression levels, as shown in *SI Appendix*, Fig. S1*B*. A paired Student's *t* test was used to evaluate statistical significance. (*C*) A structural depiction of BRAF patient mutations in the A-loop and P-loop (PDB: 4RZV). The binding of vemurafenib is indicated (green). (*D*) A time-dependent evaluation of KinCon dynamics 8 and 24 h post-transfection. The effects of PLX8394 (1 μM; 15 min) on BRAF* dynamics have been determined. The fold increase of luminescence signals originating from the complemented *R*luc PCA–based KinCon reporter following transient overexpression in HEK293 cells for indicated time frames are shown. Immunoblotting shows expression levels of endogenous and overexpressed BRAF proteins (±SEM from at least $n = 3$ independent experiments). A paired Student's *t* test was used to evaluate statistical significance. (*E*) A time-dependent evaluation of conformation dynamics using the HEK293 cell line upon exposure to 1 μM of PLX8394 (±SEM from $n = 5$ independent experiments). RLU were normalized on the untreated control. The statistical significance was assessed using the nonparametric Mann–Whitney *U* test. $*P < 0.05$, $**P < 0.01$, and $***P < 0.001$. n.s., nonsignificant.

dose-dependent lead molecule exposure on the expression-corrected conformation states (Fig. 2*B*). We detected no major alterations of the bioluminescence signal with the wild-type KinCon reporter. The most prominent effects in driving BRAF to a more closed conformation were evident with the paradox breaker PLX8394 and with encorafenib. No major change of the bioluminescence signal was detectable with the Y472C mutation in the P-loop and with the intermediate kinase–activating BRAF mutation L597V (Fig. 2*B*). Both amino acid residues are not in direct contact with BRAFi; L597V is too far away, and the side chain of Y472C points away from the ligand. In contrast, the amino acid substitutions G466V and N581S, which we tested in further experiments, are in contact with the BRAFi (Fig. 2*C*). Furthermore, we present evidence that drug-driven changes of BRAF wild type and mutant (BRAF*) KinCon dynamics correlate with the inhibitory effect of PLX8394 on downstream P-MEK levels upon transient overexpression of flag-tagged BRAF variants (*SI Appendix*, Fig. S2 *A* and *B*). The different BRAF mutants show different basal activities, as we have noted in Fig. 1*D*, showing high, intermediate, low, and no phosphotransferase activity.

Prior to focusing on G466V and N581S BRAF mutants, we characterized BRAF-V600E KinCon reporter features. We quantitatively measured BRAF and BRAF-V600E KinCon dynamics after 8 and 24 h of transient overexpression of the reporter in HEK293 cells. In total, 8 h of overexpression was sufficient to detect KinCon dynamics (Fig. 2*D*). However, at this stage, expression of the KinCon could not been tracked using immunoblotting. Threefold prolongation of the expression time (24 h) caused an ∼24-fold increase of the dynamic KinCon signal (Fig. 2*D*). Next, we recorded the time-dependent impact of PLX8394 exposure on the closing of the BRAF-V600E reporter. It is evident that BRAFi exposure promotes an immediate closing event within the first minute of exposure (Fig. 2*E*). With the BRAF-V600E KinCon reporter protein, we confirmed PLX8394-driven kinase dynamics in another cell system which is suitable for cell transformations. In the transformation assays, we demonstrated the selectivity of PLX8394 in preventing BRAF-V600E–induced cell transformation, as predicted (*SI Appendix*, Fig. S3 *A* and *B*). Next, we decided to perform KinCon reporter assays with different luciferase PCAs to compare the impact of pathway activation and drug binding on BRAF and BRAF-V600E kinase dynamics. We observed that KinCon reporters utilizing alternative luciferase fragments for the PCA (52, 53) show differences in the tested dynamic properties (*SI Appendix*, Fig. S4 *A* and *B*).

Downloaded by guest on December 15, 2020

BRAFi Affect KinCon Dynamics, Kinase Signaling, and Cancer Proliferation. Non-V600E mutations account for more than 50% of the identified mutations in NSCLC when compared with melanoma (24). We observed that some of these non-V600E patient mutations revealed differences in the effectiveness of the four tested BRAFi in the KinCon reporter recordings. Thus, we first analyzed $BRAF^{N581S}$-directed downstream signaling. Second, we validated KinCon-based drug efficacy predictions for the BRAF mutation G466V in proliferation assays using patient-derived lung cancer cell lines. According to the recent study of Chang and colleagues (25), the most frequently mutated sites besides V600 are indeed found at the position G466, G469, N581, D594, and K601 in lung adenocarcinoma (Fig. 2*A*). Interestingly, dabrafenib had no impact on the opened $BRAF^{N581S}$ conformation. Thus, we repeated the KinCon recordings with increasing doses of dabrafenib and PLX8394. In contrast to dabrafenib, we observed an immediate BRAF-N581S KinCon closing effect with the lowest dose of 1 nM PLX8394 (Fig. 3*A*). We validated this observation using HA-tagged BRAF constructs. Despite the low phosphotransferase activities of $BRAF^{N581S}$, which was evident in the ERK1/2 phosphorylation pattern, we observed efficient $BRAF^{N581S}$ kinase inhibition with the lowest PLX8394 concentration tested (10 nM; when compared with V600E and K601E mutants). However, the efficacy of dabrafenib inhibition of $BRAF^{N581S}$ was significantly lower (Fig. 3*B* and *SI Appendix*, Fig. S5 *A* and *B*). One possible structural explanation is that in contrast to encorafenib and PLX8394, the BRAFi dabrafenib misses the solvent protrusions, which might be relevant for drug binding and drug-mediated $BRAF^{N581S}$ KinCon change and inhibition (*SI Appendix*, Fig. S5*C*).

Next, we repeated KinCon measurements with the G466V mutation, which actually showed the strongest fold increase in driving the opened KinCon back to a more closed conformation (Fig. 2*B*). KinCon profiling with all four BRAFi showed major efficacy differences (Fig. 3*C*). We observed that clinically used vemurafenib and dabrafenib showed less efficacy in driving BRAF-G466V KinCon back into a more closed conformation in comparison to the paradox breaker PLX8394 (currently in preclinical trials) and the U.S. Food and Drug Administration (FDA)-approved BRAFi encorafenib. Thus, we used the NSCLC cell line H1666 carrying this BRAF genotype to compare the effect of single BRAFi exposures on cancer cell proliferation. We confirmed our predictions that 1 μM encorafenib and PLX8394 are indeed more efficient in reducing BRAF-G466V cancer cell proliferation (with H1666 cells; Fig. 3*D*). Indeed, BRAF-G466V downstream signaling has recently been shown to be effectively reduced by PLX8394 exposure in H1666 cells (54).

We also analyzed wild-type BRAF. We observed no major impact of vemurafenib, encorafenib, and PLX8394 on indicated BRAF conformations in KinCon profiling experiments in HEK293 cells (Fig. 2*B* and *SI Appendix*, Fig. S6*A*). In proliferation experiments with the NSCLC cell line A549 (wild-type BRAF, KRAS-G12S), we observed an inhibition of cell proliferation upon dabrafenib treatment (*SI Appendix*, Fig. S6*B*), which has been previously reported by others (55, 56). The other BRAFi had no inhibiting effect (*SI Appendix*, Fig. S6*B*). Next, we started to correlate BRAF-V600E KinCon dynamics with

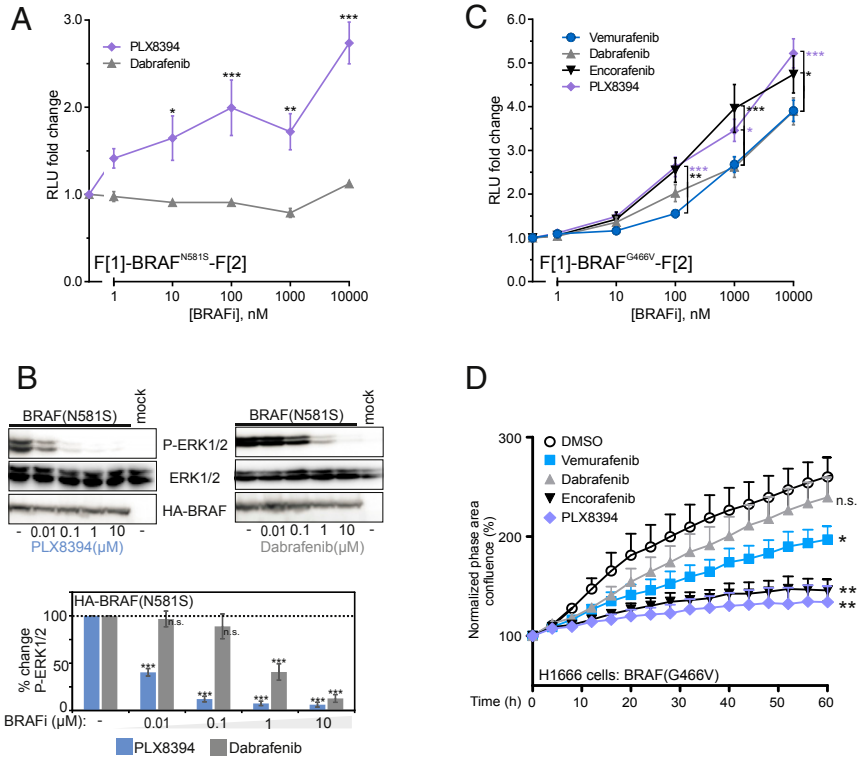

Fig. 3. Correlation of KinCon dynamics, downstream signaling, and cancer cell proliferation. (*A*) The impact of dabrafenib and PLX8394 exposure on the BRAF-N581S KinCon reporter. The quantification from at least $n = 4$ independent experiments is shown (±SEM; HEK293 cells). (*B*) The determination of P-ERK1/2 following transient expression of indicated HA-tagged BRAF mutants upon dabrafenib or PLX8394 exposure (1 h) in HEK293 cells. The quantification is from at least $n = 5$ independent experiments (±SEM). (*C*) The impact of vemurafenib, dabrafenib, encorafenib, and PLX8394 exposure on the BRAF-G466V KinCon reporter. The quantification is from $n = 10$ independent experiments (±SEM). (*D*) Shown are proliferation experiments of the H1666 cell line (BRAF-G466V mutation) following BRAFi exposure (1 μM) (±SEM; $n = 4$). Two-way ANOVA (*D*) or paired Student's *t* test (*A*–*C*) was used to evaluate statistical significance. $*P < 0.05$, $**P < 0.01$, $***P < 0.001$. n.s., nonsignificant.

Downloaded by guest on December 15, 2020

proliferation profiles. By using the patient-derived and BRAF-V600E–harboring melanoma cell line A2058, we demonstrated that vemurafenib shows the weakest effect on BRAF-V600E KinCon closing (*SI Appendix*, Fig. S6*C*) and is less efficient in reducing cancer cell proliferation when compared with PLX8394, dabrafenib, and encorafenib (*SI Appendix*, Fig. S6*D*). These data underline that the KinCon reporter platform can be used to predict efficacies of V600E mutation–specific RAF kinase inhibitors.

Next, we wanted to tackle the question of whether the KinCon concept can be extended to other members of the kinase superfamily. We selected 18 protein kinases with critical cellular functions, including kinases with and without predicted CREs (*SI Appendix*, Figs. S7 and S8), to extend the KinCon reporter platform. The selected kinases (marked in red in Fig. 1*A*) are members of different kinase families. The closed conformation of autoinhibitory proteins occasionally requires that the original protein termini are brought into vicinity (9, 13, 36–38, 42, 57). We utilized this fact and fused this handpicked collection of kinases N-terminally with fragment 1 (F[1]-) and C-terminally with fragment 2 (-F[2]) of the *R*luc-based PCA as illustrated in Fig. 1*B* (13, 48, 58). We performed overexpression experiments of the KinCon reporter collection in HEK293 cells. Following transient expression for 48 h, we observed a broad range of bioluminescence signals which originate from more or less effective complementation of the *R*luc PCA fragments and differences in reporter expression levels (Fig. 4*A* and *SI Appendix*, Fig. S8*B*). On the left side of Fig. 4*A*, we highlight the domain organization of the selected kinases and indicate predicted CREs/AIM. It was evident from the KinCon reporter experiment that many of the tested kinases show bioluminescence signals, indicating a closed conformation. At this stage, we cannot specify which activity state might be represented.

MEK and PKAc KinCon Reporter Dynamics. We selected the two well-studied kinases, MEK and protein kinase A (PKA), from the set of KinCon reporters for the further characterization of their dynamic properties (9, 39, 40). Overall, PTMs, mutations, proteolytic processing, molecular interactions, and target-oriented drugs are involved in modulating kinase activities/dynamics. Here, we tested the impact of MEK mutations and second messenger (cAMP)-triggered PKA activation on KinCon reporter dynamics. We started by analyzing conformation dynamics of another kinase member of the MAPK pathway, the MAPK MEK1/2 (59). Currently, the combination therapy using BRAF- and MEK-specific inhibitors is the standard of care, especially for BRAF-mutant melanoma patients (60). The MAPK MEK1/2 are dual-specificity kinases and downstream targets of RAF (Fig. 4*B*) (40). MEK kinases are small in size, but they still contain an N-terminal "negative regulatory region" (*SI Appendix*, Fig. S7) that is involved in stabilizing the inactive kinase conformation (40). In contrast to BRAF, MEK is less frequently mutated (40). Nevertheless, we integrated the MEK1 patient mutations K57E, K57N, and P124S (40, 61). All point mutations display different efficacies in opening and presumably activating the MEK1 KinCon reporter (Fig. 4*B*).

Furthermore, we wanted to test the possibility of monitoring GPCR signaling by recordings of KinCon dynamics. We therefore selected the second messenger–sensing PKA for KinCon analyses. The mechanism of PKA activation is one of the most studied examples for protein allostery and small-molecule:protein interactions (39). This is based on the physical interaction between a cAMP-sensing PKA regulatory subunit (R) dimer and two catalytic PKA subunits (PKAc, C). This PPI actually locks the enzyme in its inactive state (39, 62). cAMP binding to R subunits causes a conformational change and leads to PKA holoenzyme disassembly and C activation (Fig. 4 *C*, *Left*). Interestingly, C subunits contain AIM elements which may contribute to PKA dynamics upon cAMP-initiated change of R subunit interactions (*SI Appendix*, Fig. S8). Here, we show that C subunit activity changes can also be studied using the KinCon reporter

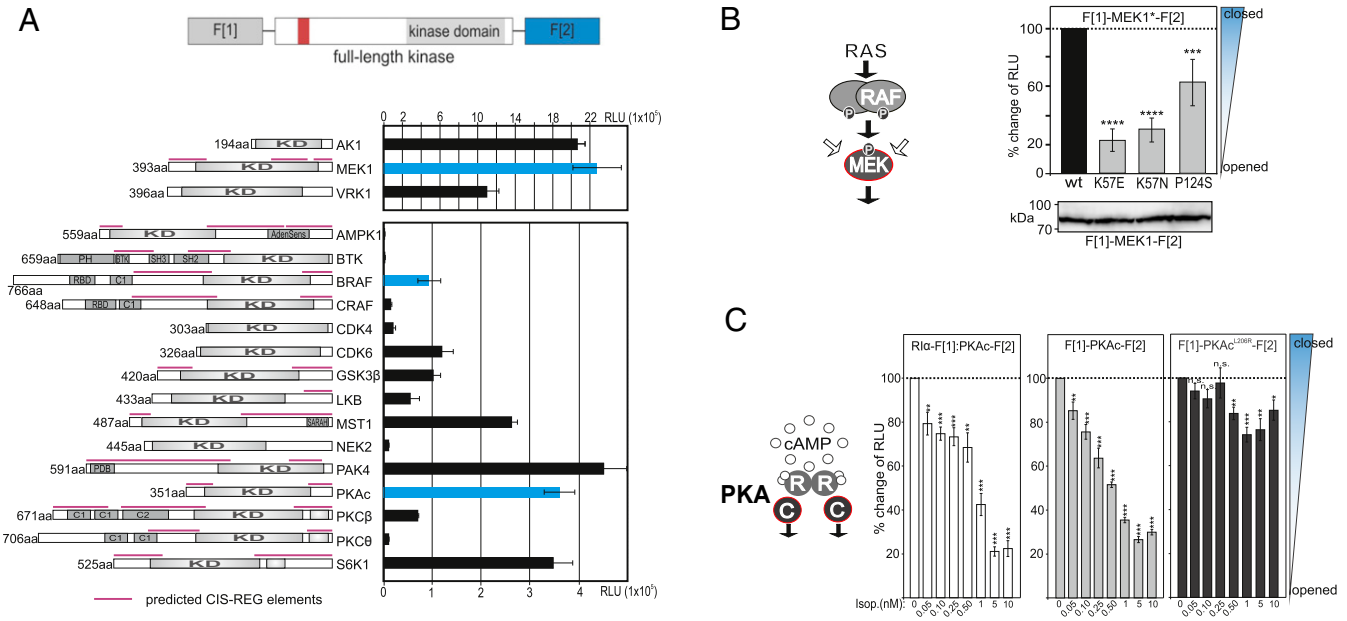

Fig. 4. KinCon reporter platform. (*A*) The domain organization of the KinCon construction principle is shown. KinCon reporter conformations were measured using transiently transfected HEK293 cells. A schematic modular illustration highlights predicted and tested CREs. Selected KinCon reporters for the presented dynamic studies are shown in blue. RLU, relative light units (a representative experiment, SD from triplicates). (*B*) An illustration of the RAS-RAF-MEK pathway. F[1]-MEK1*-F[2] conformations (wild-type [wt] and indicated mutations [*]) were measured using transiently transfected HEK293 cells (±SEM; $n = 5$ independent experiments). (*C*) The activation cycle of PKA holoenzymes is shown. F[1]-PKAc*-F[2] conformations (wt and the PKAc-L206R mutant) and RIa:PKAc (*C*) interactions were measured following Isoproterenol exposure of HEK293 cells expressing beta-2 adrenergic receptors (±SEM; $n = 6$ independent experiments). $^*P < 0.05$, $^{**}P < 0.01$, $^{***}P < 0.001$. n.s., nonsignificant.

Downloaded by guest on December 15, 2020

principle. Merely the wild-type PKA C subunits, which bind to endogenous cAMP-sensing regulatory PKA subunits [in contrast to the R subunit binding–deficient L206R PKAc mutant (63)], can be activated and give similar results as previously established PKA PPI reporters (48) following beta-2 adrenergic receptor–mediated cAMP mobilization using isoproterenol (Fig. 4*C*). These data underline that the cAMP-dependent activity status of this kinase can be tracked using the cell-based KinCon reporter system.

Nonkinase Conformation Reporter. We selected well-described proteins without enzymatic activity but with reported alternating protein conformations in order to show that the conformation reporter principle can be extended to other protein family classes (*SI Appendix*, Fig. S9*A*). We quantified closed protein conformations of the cytoskeletal protein Merlin, which acts as tumor suppressor protein and is involved in Neurofibromatosis type II (*SI Appendix*, Fig. S9*B*) (64). Furthermore, we managed to quantify a closed conformation of the Neural Wiskott-Aldrich syndrome protein N-WASP (65). Finally, we constructed a functional conformation reporter for the Serine/threonine-protein phosphatase 2A (PP2A) 65 kDa regulatory subunit A isoform alpha (PR65). The PR65 PP2A subunit serves as a dynamic scaffold for the coordinated assembly of the catalytic (C) and regulatory (B) subunits (*SI Appendix*, Fig. S9*B*). For the latter one, patient mutations have been identified (66). We showed that PR65 reporter with one selective mutation found in patients with intellectual disability show differences in its conformation upon testing of varying cell densities of standard cell lines (*SI Appendix*, Fig. S9 *C* and *D*).

Discussion

This study has established a flexible and extendable biosensor platform to record protein conformation rearrangements of full-length protein kinases in real time. The complexity of kinase regulation, missing full-length structures, the high frequency of disease mutations, and, thus, the attractiveness as a therapeutic target requires new means for monitoring kinase conformations upon drug binding in the living cell. In this study, we analyzed the impact of molecular interactions, patient mutations, and small-molecule occupancy on adjustable kinase conformations. We demonstrated that the systematic profiling of mutation:drug combinations in an intact cell setting has the potential to provide auxiliary mechanistic understanding of kinase drug specificities. Moreover, it may facilitate the choice of which lead molecule or FDA-approved drug provides the highest efficacy for a defined kinase mutant in the cellular setting. We hypothesize that widespread analyses of KinCon:drug interactions assist in identifying patient mutation–specific and thus more effective kinase inhibitors.

Here, we would like to refer to publications which address the use of BRAFi in non-V600 BRAF-carrying lung cancers and model systems. Firstly, the team of David Planchard reviewed the less-convincing therapy responses of the specific BRAFi vemurafenib and dabrafenib in treating patients with non-V600 BRAF NSCLC in the past year (table 2 in ref. 24). It is evident from our KinCon profiling that vemurafenib and dabrafenib indeed showed the weakest impact of conformation change when compared with encorafenib and the paradox breaker in clinical trials PLX8394. Secondly, it is of interest in this context that Trever Bivona's group reported how new types of BRAFi are effective in inhibiting certain non-V600 lung adenocarcinoma models. It was shown by using different patient cells lines that PLX8394 is much more effective than vemurafenib in inhibiting growth of the BRAF-G466V harboring cell lines H1666 and Cal-12T, respectively. This is in agreement with our reporter profiling. As predicted via KinCon, the impact of inhibiting cell growth is minor with both inhibitors in the H2087 cell line (L597V mutation) (54). These observations underline that patient-mutation–harboring BRAF KinCon has the potential to predict drug efficacies. In the first instance, this is relevant for selection of the correct lead molecule for the right kinase mutation. However, we would like to underline that in addition to clinical trials using single kinase inhibitors, numerous kinase-inhibitor combination therapies are under clinical investigation. In this context, KinCon may become an asset for the stratification of genotyped patient populations for clinical trials. This would elevate the success rate for bringing "personalized" kinase inhibitor mixtures into the clinic.

In general, this cell-based method has several advantages when compared with conventional kinase profiling methods that focus on recombinant kinase domain functions/activities and deal with cell lysates and/or selectively with ATP-competitive kinase inhibitors (4, 67–69). First, we provide a tool to analyze full-length kinases in their native cellular environment. Second, the sensitivity of the luciferase-based KinCon reporter allows analyses at expression levels below the endogenous proteins (Fig. 2*D*). Third, the assay has the potential to become suitable for testing/identifying unique classes of allosteric kinase modulators for specific kinase families. Finally, the simplicity and reproducibility of the test system makes it easily adaptable for the systematic profiling of mutation:drug combinations in intact cells. In order to generate a functional conformation reporter, structural information is useful. The PCA fragments need to be brought into close proximity to allow complementation of functional reporter activity. Consequently, there is a size restriction. Most kinases contain additional domains with diverse types of functions. Thus, the generation of KinCon reporters, which are based on a multidomain polypeptide chain may be challenging. Furthermore, one should test if tagging interferes with enzyme functions, molecular interactions, and/or the localization of the fusion protein/reporter. Last but not least, membrane-spanning domains might complicate the generation of a functional KinCon reporter. In addition, the luminescence signal lifetime and the low photon emission rates limit the applicability of *R*luc PCA–based reporter strategies for single-cell studies (48).

Finally, yet importantly, we present evidence that the reporter principle can be extended to other autoinhibitory proteins without enzymatic activity which are difficult to target in the *in vivo* setting. Pseudokinases might fall under this class of proteins. We propose that KinCon could become relevant for recording and perturbing pseudoenzyme functions which are challenging to track by the use of conventional readouts (70, 71). Therefore, we believe that the reporter system has the potential to provide additional information for different aspects of drug discovery. Moreover, it opens new avenues to target critical signaling node functions, which depend on the transformation of cis-regulatory protein conformations. This is a general phenomenon which is not restricted to the kinase family.

Materials and Methods

Reagents. The reagents used included PLX4032 (vemurafenib; MedChemExpress, HY-12057), LGX818 (encorafenib; MedChemExpress, HY-15605), GSK2118436A (dabrafenib; Selleckchem, S2807), PLX8394 (MedChemExpress, HY-18972), Benzyl-coelenterazine (Nanolight, 301), and human EGF (Alomone Labs, E-100).

Cell Culture and Antibodies. HEK293 cells were grown in Dulbecco's Modified Eagle Medium (DMEM) supplemented with 10% fetal bovine serum (FBS). Transient transfections were performed with Transfectin reagent (Bio-Rad, 1703352). The lung cancer cell lines A549 (ATCC CCL-185) and H1666 (ATCC CRL-5885) were grown in Roswell Park Memorial Institute media (RPMI), the melanoma cell line A2058 (ATCC CRC-11147) in DMEM. The media was supplemented with 10% FBS and 10 mM N-2-hydroxyethylpiperazine-N-ethanesulfonic acid (Hepes). Quail embryo fibroblasts (QEF) were grown in Avian cell culture medium. DNA transfection was mediated using the calcium phosphate method. Primary antibodies used were the mouse anti-*R*luc antibody directed against *R*luc-F[1] (Chemicon, #MAB4410), mouse anti–HA-tag

Downloaded by guest on December 15, 2020

(Covance, MMS-10P), mouse anti-BRAF (Santa Cruz, F-7: sc-5284), mouse anti-MEK1/2 (Cell Signaling, 4684S), rabbit phospho-MEK1/2 (Ser217/221) (Cell Signaling, 9154), and rabbit anti–P-ERK1/2 (Cell Signaling, 9101).

Expression Constructs. The *R*luc-PCA–based hybrid proteins RI-α-F[1] (RI-α: NM_001278433) and PKAc-F[2] (PKAc: NM_002730.1) have been designed as previously described (58). Following PCR amplification of the human BRAF gene (BRaf: NM_004333.4, Addgene plasmid 40775), we fused the KinCon reporter N-terminally with -F[1] and C-terminally with -F[2] of the *R*luc, *G*luc, and Nluc-PCA (pcDNA3.1 backbone vector). We inserted interjacent 10-amino-acid linkers. A site-directed mutagenesis approach has been used to generate the BRAF (G466V, G469A, Y472C, N581S, D594G, L597V, V600E, V600K, V600R, and K601E) amino acid substitutions. The identical cloning approach has been used to generate the *R*luc-PCA–based hybrid proteins of MEK (MEK1: NM_002755.3), CRAF (CRaf: NM_002880.3), PKAc (PKAc: NM_002730.1), PKC-β (NM_212535.2), PKCθ (PKCθ: L07032.1), CDK4 (CDK4: NM_000075), CDK6 (NM_001259), and PR65 (NM_014225) and were mutated using a site-directed mutagenesis approach. To generate the *R*luc-PCA–based fusion proteins of AK1 (AK1: NM_000476.2), VRK1 (VRK1: NM_003384.2), AMPK1 (AMPK1: NM_006251.5), BTK (BTK: NM_001287345.1), GSK3-β (GSK3β: NM_001146156.1), LKB (LKB: NM_000455.4), MST1 (MST1: NM_006282.4), NEK2 (NEK2: NM_002497.3), PAK4 (PAK4: NM_005884.3), S6K1 (S6K1: NM_003161.3) N-WASP (N-WASP: NM_003941.3), PR65 (NM_014225), and NF2 (NF2: NM_000268.3), we ordered customized genes synthesized by Eurofins and cloned the coding region into the pcDNA3.1 vector with N-terminally located –F[1] and C-terminally located –F[2]. The HA-tag was inserted N-terminally of BRAF* by PCR and cloned into the pcDNA3.1 vector using restriction enzymes. For the construction of replication-competent RCASBP (A) vector (pRCAS)-HA-MYC, the human *MYC* coding region was amplified by PCR using complementary DNA derived from SW-480 cells and primers providing a HA tag for the N terminus of the expressed MYC protein. The PCR product was ligated into the *Cla*I site of pRCAS. The coding region of human $BRAF^{V600E}$ was amplified from the plasmid pcDNA3.1-FLAG-$BRAF^{V600E}$ using primers providing a C-terminal HA tag. The PCR product was then inserted into the unique *Cla*I site of the pCRNCM vector, a replication-defective derivative of pRCAS (72), yielding the construct pCRNCM-FLAG-$BRAF^{V600E}$-HA. To create the intramolecular reporter construct pCRNCM-F1-$BRAF^{V600E}$-F2, a 3,332-base-pair *Nco*I/*Dra*I DNA fragment encompassing the F1-$BRAF^{V600E}$-F2 coding region was excised from pcDNA3.1-F1-$BRAF^{V600E}$-F2, inserted into the adaptor plasmid pA-CLA12NCO as described (73), and, from there, transferred into the *Cla*I site of pCRNCM. The coding regions of human BRAF and BRAF-V600E were amplified from the plasmids pcDNA3.1-FLAG-BRAF and pcDNA3.1-FLAG-BRAF-V600E (http://addgene.org), respectively, using primers providing a C-terminal HA tag. The PCR products were then ligated into the ClaI site of pRCAS.

Luciferase PCA Analyses. Cells were grown in DMEM supplemented with 10% FBS. Indicated versions of the *R*luc PCA–based reporter were transiently overexpressed in 24-well or 12-well plate formats. The drug exposure experiments were initiated 24 or 48 h post-transfection. The growth medium was partially removed, and BRAFi were added with the final concentrations as indicated in the figure legends. To measure the dose-dependent effect of the lead molecules on the intramolecular *R*luc PCA reporter, we treated cells with two different concentrations for 1 h. For the luciferase PCA measurements, the growth medium was carefully removed, and the cells were washed with phosphate-buffered saline. Cell suspensions were transferred to 96-well plates and subjected to luminescence analysis using either the PHERAstar FSX (BMG Labtech) or the LMaxTM-II-384 luminometer (Molecular Devices). Luciferase luminescence signals were integrated for 10 s following the addition of the *R*luc substrate benzylcoelenterazine (Nanolight, 301). For the PP2A conformation reporter assays, HEK293 cells were grown in DMEM supplemented with 10% FBS at two different cell densities: low-density cells were seeded at 50,000 cells/well and high-density cells at 100,000 cells/well in a 24-well-plate format. They were transiently overexpressed with the indicated versions of the Rluc-PP2A conformation reporter for 48 h post-transfection. For the time-dependency experiments, HEK293 cells were seeded in 24-well plates (90,000 cells/well), and after 1 d, they were transfected with the KinCon reporters BRAF-wt or BRAF-V600E (50 ng DNA pro well). Cells were treated with 1 μM PLX8394 for indicated time points and subjected to PCA measurements 48 h post-transfection.

MEK and ERK Phosphorylation. Following overexpression of indicated KinCon constructs or expression constructs for Flag-tagged BRAF in HEK293 cells, we directly determined the phosphorylation status of ERK1/2 and MEK1/2 with indicated antibodies. We treated HEK293 cells with indicated BRAFi or EGF, exchanged the medium, and added the Laemmli sample buffer.

Cell Transformation Assay. QEF were prepared from 9-d-old embryos of *Coturnix japonica* (73). To deliver the eukaryotic expression vectors (pcDNA3.1) or the retroviral DNA constructs (RCAS) into QEF, each 6×10^5 cells were seeded onto six well plates and transfected each with 2.0 μg DNA using the calcium phosphate method. Colony assays from transfected cells, which have been passaged five times, were done as described (73). Each of the 25,000 cells were suspended in cloning agar onto MP-12 dishes. For the inhibitor treatment, 25,000 cells were suspended in cloning agar containing PLX8394 onto MP-12 dishes, resulting in final concentrations of 4 μM. To monitor protein expression, immunoblot analysis was done using antibodies directed against BRAF, (Santa Cruz), *R*luc-F[2] (Merck), the HA-tag (Covance), or tubulin-α (Merck).

Cell Proliferation Assays. The lung cancer cell lines A549, H1666, and A2058 were seeded in a 96-well plate at a density of 10,000 to 15,000 cells/well and cultured overnight. One day later, BRAFi were added at a final concentration of 1 μM, and cell growth was monitored for 60 h using the Incucyte S3 Live-Cell Analysis system (Essen Bioscience). Four images per well were taken at 4-h intervals. Normalized confluence area was processed using the Incucyte S3 Sofware (Essen Bioscience).

In Silico Predictions. All human kinases were retrieved from the Uniprot database (https://www.uniprot.org/). Kinases were assigned to their respective classes. The sequences of all kinases were then processed by the Cis-regPred server (http://aimpred.cau.ac.kr) for the presence of CREs (36). *SI Appendix*, Table S1 shows the number of CREs identified within each kinase sequence. To visualize the relationship of kinase similarity with the presence of CREs, we calculated all pairwise sequence identities after individual pairwise alignments within each class using *mafft* with the L-ins-I strategy. Subsequently, all screened kinases were mapped into the phylogenetic tree of the human kinome using the web-based tool KinMap (http://www.kinhub.org/kinmap) (43).

Statistical Analyses. Data were examined for Gaussian distribution using the Kolmogorov–Smirnov normality test. Non-Gaussian–distributed data were analyzed using the nonparametric Mann–Whitney *U* test. Besides two-way ANOVA, paired Student's *t* tests were used to evaluate statistical significance. Values are expressed as the mean ± SEM or ± SD as indicated. Significance was set at the 95% confidence level and ranked as $P < 0.05$, $P < 0.01$, and $P < 0.001$.

Data Availability. Data supporting the findings of this study are available within the article and its *SI Appendix* files.

ACKNOWLEDGMENTS. We thank Sonja Beiler, Anja Reintjes, and Josh Insole for technical support and Gabi Reiter for management support. This work was supported by grants from the Austrian Science Fund (P27606, P30441, and P32960) and the Tyrolean Cancer Society.

1. E. D. Fleuren, L. Zhang, J. Wu, R. J. Daly, The kinome 'at large' in cancer. *Nat. Rev. Cancer* **16**, 83–98 (2016).
2. K. S. Bhullar *et al.*, Kinase-targeted cancer therapies: Progress, challenges and future directions. *Mol. Cancer* **17**, 48 (2018).
3. A. J. Sabnis, T. G. Bivona, Principles of resistance to targeted cancer therapy: Lessons from basic and translational cancer biology. *Trends Mol. Med.* **25**, 185–197 (2019).
4. F. M. Ferguson, N. S. Gray, Kinase inhibitors: The road ahead. *Nat. Rev. Drug Discov.* **17**, 353–377 (2018).
5. R. Yaeger, R. B. Corcoran, Targeting alterations in the RAF-MEK pathway. *Cancer Discov.* **9**, 329–341 (2019).
6. Z. Karoulia, E. Gavathiotis, P. I. Poulikakos, New perspectives for targeting RAF kinase in human cancer. *Nat. Rev. Cancer* **17**, 676–691 (2017).
7. C. Wellbrock, M. Karasarides, R. Marais, The RAF proteins take centre stage. *Nat. Rev. Mol. Cell Biol.* **5**, 875–885 (2004).
8. E. Desideri, A. L. Cavallo, M. Baccarini, Alike but different: RAF paralogs and their signaling outputs. *Cell* **161**, 967–970 (2015).
9. H. Lavoie, M. Therrien, Regulation of RAF protein kinases in ERK signalling. *Nat. Rev. Mol. Cell Biol.* **16**, 281–298 (2015).
10. P. T. Wan *et al.*; Cancer Genome Project, Mechanism of activation of the RAF-ERK signaling pathway by oncogenic mutations of B-RAF. *Cell* **116**, 855–867 (2004).

Downloaded by guest on December 15, 2020

11. T. Jin *et al*., RAF inhibitors promote RAS-RAF interaction by allosterically disrupting RAF autoinhibition. *Nat. Commun.* **8**, 1211 (2017).
12. N. H. Tran, X. Wu, J. A. Frost, B-Raf and Raf-1 are regulated by distinct autoregulatory mechanisms. *J. Biol. Chem.* **280**, 16244–16253 (2005).
13. R. Rock *et al*., BRAF inhibitors promote intermediate BRAF(V600E) conformations and binary interactions with activated RAS. *Sci. Adv.* **5**, eaav8463 (2019).
14. E. M. Terrell *et al*., Distinct binding preferences between ras and raf family members and the impact on oncogenic ras signaling. *Mol. Cell* **76**, 872–884.e5 (2019).
15. E. Tiacci *et al*., BRAF mutations in hairy-cell leukemia. *N. Engl. J. Med.* **364**, 2305–2315 (2011).
16. P. Lito, N. Rosen, D. B. Solit, Tumor adaptation and resistance to RAF inhibitors. *Nat. Med.* **19**, 1401–1409 (2013).
17. M. R. Girotti, G. Saturno, P. Lorigan, R. Marais, No longer an untreatable disease: How targeted and immunotherapies have changed the management of melanoma patients. *Mol. Oncol.* **8**, 1140–1158 (2014).
18. J. Sun, J. S. Zager, Z. Eroglu, Encorafenib/binimetinib for the treatment of BRAF-mutant advanced, unresectable, or metastatic melanoma: Design, development, and potential place in therapy. *OncoTargets Ther.* **11**, 9081–9089 (2018).
19. G. Hatzivassiliou *et al*., RAF inhibitors prime wild-type RAF to activate the MAPK pathway and enhance growth. *Nature* **464**, 431–435 (2010).
20. S. J. Heidorn *et al*., Kinase-dead BRAF and oncogenic RAS cooperate to drive tumor progression through CRAF. *Cell* **140**, 209–221 (2010).
21. P. I. Poulikakos, C. Zhang, G. Bollag, K. M. Shokat, N. Rosen, RAF inhibitors transactivate RAF dimers and ERK signalling in cells with wild-type BRAF. *Nature* **464**, 427–430 (2010).
22. M. Holderfield, M. M. Deuker, F. McCormick, M. McMahon, Targeting RAF kinases for cancer therapy: BRAF-mutated melanoma and beyond. *Nat. Rev. Cancer* **14**, 455–467 (2014).
23. S. A. Forbes *et al*., COSMIC: Mining complete cancer genomes in the catalogue of somatic mutations in cancer. *Nucleic Acids Res.* **39**, D945–D950 (2011).
24. A. Leonetti *et al*., BRAF in non-small cell lung cancer (NSCLC): Pickaxing another brick in the wall. *Cancer Treat. Rev.* **66**, 82–94 (2018).
25. M. T. Chang *et al*., Identifying recurrent mutations in cancer reveals widespread lineage diversity and mutational specificity. *Nat. Biotechnol.* **34**, 155–163 (2016).
26. L. Lin *et al*., Mapping the molecular determinants of BRAF oncogene dependence in human lung cancer. *Proc. Natl. Acad. Sci. U.S.A.* **111**, E748–E757 (2014).
27. D. Planchard, B. E. Johnson, BRAF adds an additional piece of the puzzle to precision oncology-based treatment strategies in lung cancer. *Arch. Pathol. Lab. Med.* **142**, 796–797 (2018).
28. A. Noeparast *et al*., Non-V600 BRAF mutations recurrently found in lung cancer predict sensitivity to the combination of Trametinib and Dabrafenib. *Oncotarget* **8**, 60094–60108 (2016).
29. D. Frisone, A. Friedlaender, U. Malapelle, G. Banna, A. Addeo, A BRAF new world. *Crit. Rev. Oncol. Hematol.* **152**, 103008 (2020).
30. J. Kim *et al*., A dynamic hydrophobic core orchestrates allostery in protein kinases. *Sci. Adv.* **3**, e1600663 (2017).
31. J. Hu *et al*., Kinase regulation by hydrophobic spine assembly in cancer. *Mol. Cell. Biol.* **35**, 264–276 (2015).
32. J. Hu *et al*., Allosteric activation of functionally asymmetric RAF kinase dimers. *Cell* **154**, 1036–1046 (2013).
33. E. Papaleo *et al*., The role of protein loops and linkers in conformational dynamics and allostery. *Chem. Rev.* **116**, 6391–6423 (2016).
34. H. N. Motlagh, J. O. Wrabl, J. Li, V. J. Hilser, The ensemble nature of allostery. *Nature* **508**, 331–339 (2014).
35. R. G. Smock, L. M. Gierasch, Sending signals dynamically. *Science* **324**, 198–203 (2009).
36. J. H. Yeon, F. Heinkel, M. Sung, D. Na, J. Gsponer, Systems-wide identification of cis-regulatory elements in proteins. *Cell Syst.* **2**, 89–100 (2016).
37. T. Trudeau *et al*., Structure and intrinsic disorder in protein autoinhibition. *Structure* **21**, 332–341 (2013).
38. M. A. Pufall, B. J. Graves, Autoinhibitory domains: Modular effectors of cellular regulation. *Annu. Rev. Cell Dev. Biol.* **18**, 421–462 (2002).
39. S. S. Taylor, R. Ilouz, P. Zhang, A. P. Kornev, Assembly of allosteric macromolecular switches: Lessons from PKA. *Nat. Rev. Mol. Cell Biol.* **13**, 646–658 (2012).
40. C. J. Caunt, M. J. Sale, P. D. Smith, S. J. Cook, MEK1 and MEK2 inhibitors and cancer therapy: The long and winding road. *Nat. Rev. Cancer* **15**, 577–592 (2015).
41. M. J. Knape *et al*., Divalent metal ions Mg^{2+} and Ca^{2+} have distinct effects on protein kinase A activity and regulation. *ACS Chem. Biol.* **10**, 2303–2315 (2015).
42. F. Enzler, P. Tschaikner, R. Schneider, E. Stefan, KinCon: Cell-based recording of full-length kinase conformations. *IUBMB Life* **72**, 1168–1174 (2020).
43. S. Eid, S. Turk, A. Volkamer, F. Rippmann, S. Fulle, KinMap: A web-based tool for interactive navigation through human kinome data. *BMC Bioinformatics* **18**, 16 (2017).
44. G. Manning, D. B. Whyte, R. Martinez, T. Hunter, S. Sudarsanam, The protein kinase complement of the human genome. *Science* **298**, 1912–1934 (2002).
45. H. Davies *et al*., Mutations of the BRAF gene in human cancer. *Nature* **417**, 949–954 (2002).
46. H. Lavoie *et al*., Inhibitors that stabilize a closed RAF kinase domain conformation induce dimerization. *Nat. Chem. Biol.* **9**, 428–436 (2013).
47. K. Terai, M. Matsuda, Ras binding opens c-Raf to expose the docking site for mitogen-activated protein kinase kinase. *EMBO Rep.* **6**, 251–255 (2005).
48. R. Röck *et al*., In-vivo detection of binary PKA network interactions upon activation of endogenous GPCRs. *Sci. Rep.* **5**, 11133 (2015).
49. V. A. Bachmann *et al*., Gpr161 anchoring of PKA consolidates GPCR and cAMP signaling. *Proc. Natl. Acad. Sci. U.S.A.* **113**, 7786–7791 (2016).
50. Z. Yao *et al*., Tumours with class 3 BRAF mutants are sensitive to the inhibition of activated RAS. *Nature* **548**, 234–238 (2017).
51. G. Zheng *et al*., Clinical detection and categorization of uncommon and concomitant mutations involving BRAF. *BMC Cancer* **15**, 779 (2015).
52. I. Remy, S. W. Michnick, A highly sensitive protein-protein interaction assay based on Gaussia luciferase. *Nat. Methods* **3**, 977–979 (2006).
53. A. S. Dixon *et al*., NanoLuc complementation reporter optimized for accurate measurement of protein interactions in cells. *ACS Chem. Biol.* **11**, 400–408 (2016).
54. R. A. Okimoto *et al*., Preclinical efficacy of a RAF inhibitor that evades paradoxical MAPK pathway activation in protein kinase BRAF-mutant lung cancer. *Proc. Natl. Acad. Sci. U.S.A.* **113**, 13456–13461 (2016).
55. A. Del Curatolo *et al*., Therapeutic potential of combined BRAF/MEK blockade in BRAF-wild type preclinical tumor models. *J. Exp. Clin. Cancer Res.* **37**, 140 (2018).
56. M. Phadke *et al*., Dabrafenib inhibits the growth of BRAF-WT cancers through CDK16 and NEK9 inhibition. *Mol. Oncol.* **12**, 74–88 (2018).
57. R. Bayliss, T. Haq, S. Yeoh, The Ys and wherefores of protein kinase autoinhibition. *Biochim. Biophys. Acta* **1854**, 1586–1594 (2015).
58. E. Stefan *et al*., Quantification of dynamic protein complexes using Renilla luciferase fragment complementation applied to protein kinase A activities in vivo. *Proc. Natl. Acad. Sci. U.S.A.* **104**, 16916–16921 (2007).
59. R. Roskoski, Jr, MEK1/2 dual-specificity protein kinases: Structure and regulation. *Biochem. Biophys. Res. Commun.* **417**, 5–10 (2012).
60. J. J. Luke, K. T. Flaherty, A. Ribas, G. V. Long, Targeted agents and immunotherapies: Optimizing outcomes in melanoma. *Nat. Rev. Clin. Oncol.* **14**, 463–482 (2017).
61. M. E. Arcila *et al*., MAP2K1 (MEK1) mutations define a distinct subset of lung adenocarcinoma associated with smoking. *Clin. Cancer Res.* **21**, 1935–1943 (2015).
62. O. Torres-Quesada, J. E. Mayrhofer, E. Stefan, The many faces of compartmentalized PKA signalosomes. *Cell. Signal.* **37**, 1–11 (2017).
63. R. Röck, J. E. Mayrhofer, V. Bachmann, E. Stefan, Impact of kinase activating and inactivating patient mutations on binary PKA interactions. *Front. Pharmacol.* **6**, 170 (2015).
64. A. M. Petrilli, C. Fernández-Valle, Role of Merlin/NF2 inactivation in tumor biology. *Oncogene* **35**, 537–548 (2016).
65. O. Alekhina, E. Burstein, D. D. Billadeau, Cellular functions of WASP family proteins at a glance. *J. Cell Sci.* **130**, 2235–2241 (2017).
66. G. Houge *et al*., B56δ-related protein phosphatase 2A dysfunction identified in patients with intellectual disability. *J. Clin. Invest.* **125**, 3051–3062 (2015).
67. J. D. Vasta *et al*., Quantitative, wide-spectrum kinase profiling in live cells for assessing the effect of cellular ATP on target engagement. *Cell Chem. Biol.* **25**, 206–214.e11 (2018).
68. T. Anastassiadis, S. W. Deacon, K. Devarajan, H. Ma, J. R. Peterson, Comprehensive assay of kinase catalytic activity reveals features of kinase inhibitor selectivity. *Nat. Biotechnol.* **29**, 1039–1045 (2011).
69. M. Taipale *et al*., Chaperones as thermodynamic sensors of drug-target interactions reveal kinase inhibitor specificities in living cells. *Nat. Biotechnol.* **31**, 630–637 (2013).
70. J. M. Murphy, P. D. Mace, P. A. Eyers, Live and let die: Insights into pseudoenzyme mechanisms from structure. *Curr. Opin. Struct. Biol.* **47**, 95–104 (2017).
71. A. J. M. Ribeiro *et al*., Emerging concepts in pseudoenzyme classification, evolution, and signaling. *Sci. Signal.* **12**, eaat9797 (2019).
72. C. T. Quang, O. Wessely, M. Pironin, H. Beug, J. Ghysdael, Cooperation of Spi-1/PU.1 with an activated erythropoietin receptor inhibits apoptosis and Epo-dependent differentiation in primary erythroblasts and induces their Kit ligand-dependent proliferation. *EMBO J.* **16**, 5639–5653 (1997).
73. M. Hartl, A. I. Karagiannidis, K. Bister, Cooperative cell transformation by Myc/Mil(Raf) involves induction of AP-1 and activation of genes implicated in cell motility and metastasis. *Oncogene* **25**, 4043–4055 (2006).

Downloaded by guest on December 15, 2020